Extreme intra-seasonal anomalies in the Amundsen and Bellingshausen sea-ice area, Antarctica, during the austral winter

Fabio Ullmann Furtado de LIMA, Leila M. Véspoli de CARVALHO

Department of Atmospheric Sciences, University of São Paulo, Rua do Matão 1226, São Paulo-SP 05508-090, Brazil
E-mail: fufl@model.iag.usp.br

ABSTRACT. We examine the role of the propagation of atmospheric mid-latitudes wave trains in modulating the Amundsen and Bellingshausen sea-ice area (SIA), Antarctica, on intra-seasonal timescales (20–100 days). Spectral analysis of passive microwave estimates of SIA in the Amundsen and Bellingshausen Seas for 1979–2004 shows significant peaks on intra-seasonal timescales. Previous studies have suggested that variations in SIA are linked to disturbances in atmospheric circulation and sea surface temperature. We show that extreme SIA anomalies on intra-seasonal timescales lag the propagation of subtropical wave trains in the Southern Hemisphere by approximately 10–15 days. The sign of the SIA anomaly depends on the phase of the wave. We present evidence that the number of disturbances that cause extreme anomalies of SIA on intra-seasonal timescales has increased in the last 14 years.

1. INTRODUCTION

There is general consensus that the Antarctic sea ice responds to atmospheric variability on a variety of timescales. Walker (1923, 1924) pioneered the observations on the relationships between the limit of the Antarctic sea ice and variations in sea-level pressure, storm tracks and the Southern Oscillation Index (SOI). Later, Simmonds and Jacka (1995) examined the links between SOI and sea ice in several sectors of Antarctica. They found strong relationships between ice extent in the southeast Indian Ocean in April–October and the SOI of the previous 12 months. More recently, Harangozo (2000) showed that the El Niño–Southern Oscillation (ENSO) teleconnection patterns and related changes in the meridional circulation can influence sea-ice extent and surface air temperature west of the Antarctica Peninsula (Bellingshausen Sea). In addition to ENSO, other atmospheric low-frequency modes can influence the interannual variability of the Amundsen and Bellingshausen sea-ice area (SIA). For instance, the Antarctic dipole, characterized by a quasi-stationary wave, has an out-of-phase relationship with sea-ice anomalies and temperature over the Bellingshausen and Weddell Seas (Yuan and Martinson, 2001; Renwick, 2002).

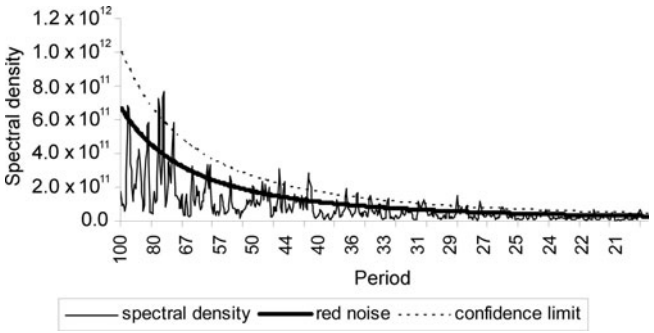

Fig. 1. Spectral density of daily Amundsen and Bellingshausen SIA (km^2). Thick (thin) solid (dashed) line represents the background red noise (95% confidence limit) spectrum. Only the intra-seasonal (20–100 days) band is shown for simplification. Hamming window ($L = 5$) was applied to the spectrum.

White and Peterson (1996), using data from a variety of observational techniques, identified significant interannual variations in the atmospheric pressure at sea-ice level, wind stress and sea-ice extent over the Southern Ocean. This system of coupled anomalies, known as the Antarctic Circumpolar Wave (ACW), propagates eastward, takes 8–10 years to encircle the pole and plays an important role in climate regulation and dynamics both within and beyond the Southern Ocean. The authors showed that the ACW can generate anomalies in the sea-ice extent, such as the intense ice retraction observed in the summers of 1988–91 in the Bellingshausen Sea.

Baba and Wakatsuchi (2001) found an eastward-propagating pattern on intra-seasonal timescales (5–30 days) with zonal wavenumber 2–4 in the marginal ice concentration around Antarctica. Baba and others (2006) applied complex empirical orthogonal functions (CEOFs) to examine the relationships between intra-seasonal (5–30 days) daily sea-ice concentration (1991–2001), ice-drifting velocity and meridional and zonal wind velocity at 10 m. They showed that the largest amplitudes in variability along the marginal sea-ice zone occur around West Antarctica, especially in the Amundsen and Bellingshausen Seas. The first CEOF mode indicated that the spatial phase of the meridional wind velocity precedes that of the sea-ice concentration by 90°.

Our objective is to investigate extreme intra-seasonal anomalies in the Amundsen and Bellingshausen SIA, with focus on persistence and interannual variability of the events. The relationships between the Amundsen and Bellingshausen extreme SIA on intra-seasonal timescales and the propagation of wave trains in the subtropics and extratropics of the Southern Hemisphere (SH) are also examined. We investigate the vertical structure of the atmospheric wave trains and the relationships with changes in circulation near the surface and respective response on the Amundsen and Bellingshausen sea ice.

2. DATA

Daily SIA of the Amundsen and Bellingshausen Seas is a satellite estimate from the scanning multichannel microwave radiometer (SMMR) and Special Sensor Microwave/Imager (SSM/I F-8, SSM/I F-11e, SSM/I F-13) available from

https://doi.org/10.3189/172756408784700671 Published online by Cambridge University Press

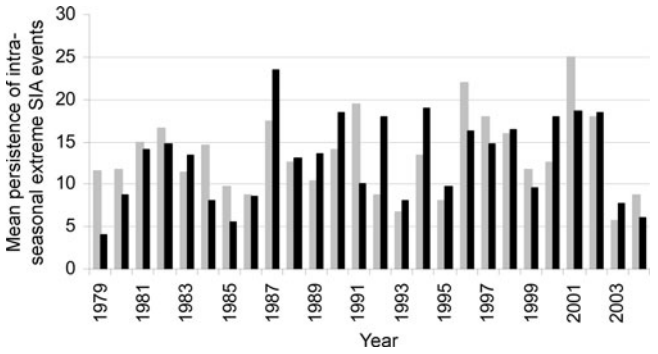

Fig. 2. Interannual variability of the mean persistence of extreme positive (black bars) and negative (grey bars) SIA_{IS} anomalies during the winter (June–September) in the Amundsen and Bellingshausen Seas.

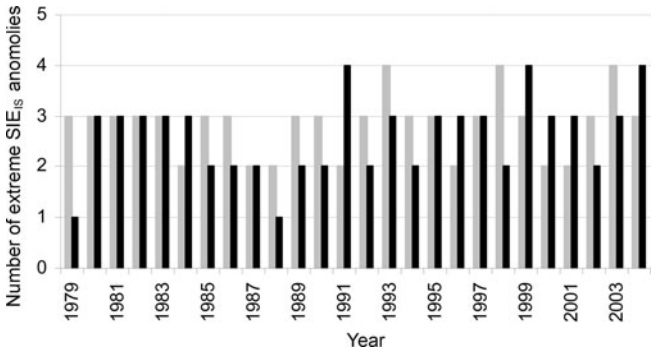

Fig. 3. Interannual variability of the number of extreme positive (black bars) and negative (grey bars) SIA_{IS} anomalies during the winter (June–September) in the Amundsen and Bellingshausen Seas. Only events persisting at least 2 days are included.

the US National Snow and Ice Data Center (NSIDC) during 1979–2004. Total ice-covered area is defined as the area of each pixel with at least 15% ice concentration, multiplied by the ice fraction (i.e. 0.15–1.00) in the pixel. Data from 1979 to 1987 were originally obtained every 2 days and were further interpolated to daily resolution.

Global daily US National Centers for Environmental Prediction/US National Center for Atmospheric Research (NCEP/NCAR) re-analysis data (Kalnay and others, 1996), with 2.5° latitude and longitude, during 1979–2004 are investigated. The following variables are examined: 200 hPa geopotential height (gpm), zonal and meridional winds at 850 and 200 hPa ($m\,s^{-1}$) and skin temperature (K). The 200 hPa geopotential height and circulation at low and high levels are used to examine the main dynamical features associated with the atmospheric disturbances that propagate toward the Antarctic Peninsula and cause variations in SIA. Skin temperature is used here as a proxy for sea surface temperature anomalies (Kalnay and others, 1996).

3. METHODS AND RESULTS

The Amundsen and Bellingshausen SIA is characterized by a very pronounced annual cycle. In addition, trends in SIA are observed in some seasons. Lima (2007) showed a negative and statistically significant SIA trend (corresponding to about $-371\,875\,km^2$ during the 1979–2004 period) for the month with minimum SIA (February) in the Amundsen and Bellingshausen Seas. Nevertheless, no statistically significant trends were found during the month of maximum extent (September). Zwally and others (2002) found negative and near-zero SIA trends during the winter and spring (1979–98) in all Antarctic oceanic sectors with the exception of the Ross Sea, which shows positive trends in all seasons. In order to identify the importance of other frequencies in the SIA spectrum, the annual cycle was removed from the data. The long-term linear trend was removed from daily data, and the SIA mean annual cycle was computed from the detrended SIA (1 January 1979 to 31 December 2004). The resulting mean annual cycle was further smoothed and removed from the detrended SIA.

The spectral density of daily Amundsen and Bellingshausen SIA anomalies indicates statistically significant peaks on intra-seasonal timescales of 20–100 days (Fig. 1). Based on this result, the Amundsen and Bellingshausen SIA were band-filtered such that only the 20–100 days band is retained. A fast Fourier transform filter was used for this purpose (e.g. Helms, 1967; Carvalho and others, 2005). Extreme intra-seasonal SIA anomalies (SIA_{IS}) were then determined based on the quartiles of the SIA_{IS} seasonal distribution. The focus of the present study is on the winter (June–September) because previous analyses (Lima, 2007) indicated that the links between atmospheric intra-seasonal variability and SIA_{IS} are stronger during this season, compared with summer. Extreme positive, equivalent to expansion, (negative, equivalent to retraction) SIA_{IS} anomalies are defined here when $SIA_{IS} \geq$ upper quartile ($SIA_{IS} \leq$ lower quartile) of the distribution of anomalies observed during June–September.

Persistence, defined as the number of consecutive days of extreme SIA_{IS}, is normally distributed with median ~12 days and interquartile range ~10 days for both positive and negative SIA_{IS} during the winter (June–September). The interannual variability of the mean persistence of winter extreme SIA_{IS} events (Fig. 2) is not stationary. During 1979–90 the lower quartile of the persistence distribution of negative (positive) SIA_{IS} extreme events is 8 days (9 days). The upper quartile of the persistence distribution of negative (positive) SIA_{IS} extreme events during 1979–90 is 16 days (15.5 days), with an interquartile range of 8 (6.5) days. During 1991–2004 the lower quartile of negative (positive) SIA_{IS} extreme events was 7 days (7 days) and the upper quartile was 19 days (16 days), yielding an interquartile range of 12 days (9 days). The increase in the interquartile range for negative anomalies (i.e. retraction of SIA) in the winter of the last 14 years is essentially due to the increase in the upper quartile after 1991, which in turn is particularly influenced by large mean persistence observed in 1991, 1996 and 2001 (Fig. 2).

The interannual variability of the number of independent extreme SIA_{IS} events during the winter with persistence $\geq$2 days is shown in Figure 3. Extreme SIA_{IS} negative and positive anomalies occur every winter, but not with the same proportion and variability. It is noteworthy that the variability in the number of intra-seasonal events increased after 1990. For instance, during 1979–90 there was no winter with more than three SIA_{IS} extreme events, either negative or positive. In the following 14 years, four SIA_{IS} extreme events occurred in approximately 42% of the winters. The increase in the number of SIA_{IS} extreme events and in the upper-quartile and interquartile range of the persistence of events may have implications for the sea-ice annual variability and trend observed in Zwally and others (2002) and Lima (2007).

https://doi.org/10.3189/172756408784700671 Published online by Cambridge University Press

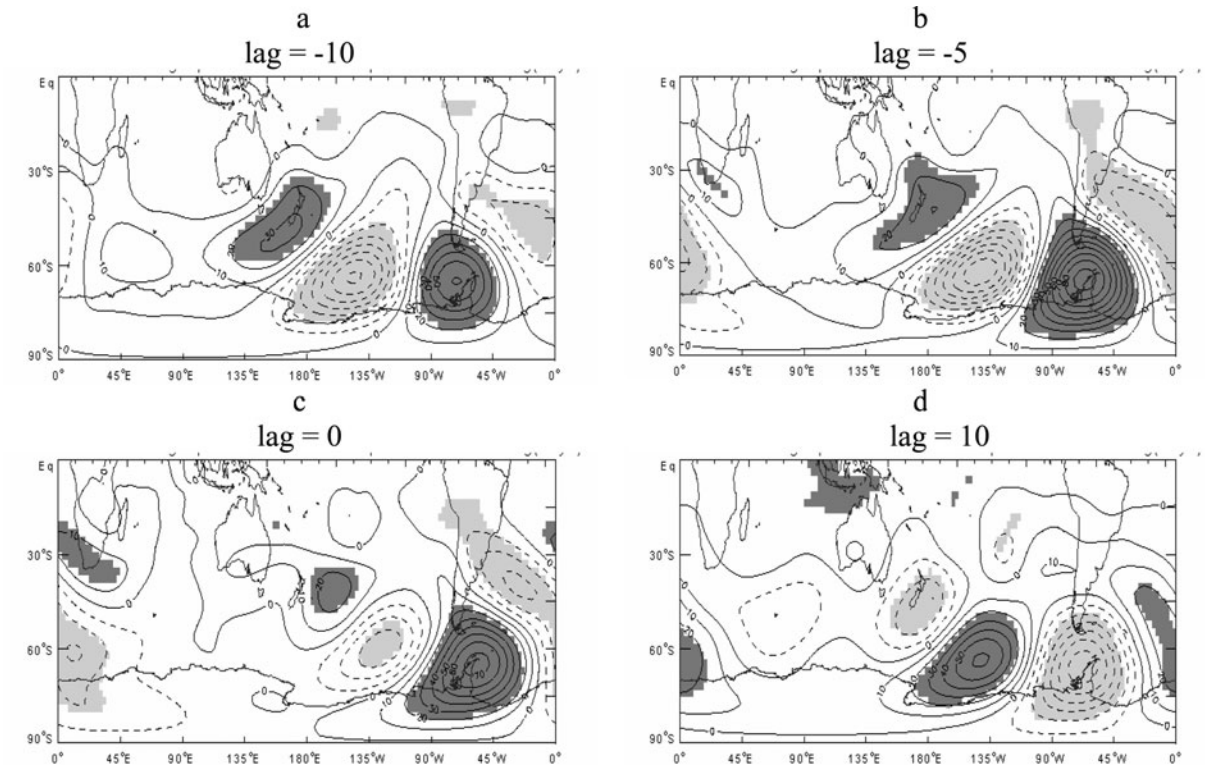

Fig. 4. Lag composites of the 200 hPa geopotential height (gpm) for dates with negative SIA_{IS} anomalies in the Amundsen and Bellingshausen Seas: (a) 10 days before the event; (b) 5 days before the event; (c) along with the event; and (d) 10 days after the event. Solid (dashed) lines indicate positive (negative) values starting with 200 gpm (–200 gpm) with interval 10 gpm. Shades show statistically significant anomalies at 5% significance level. Number of degrees of freedom (DOF) is 70, which corresponds to the number of independent events minus 2.

The statistical significance in the difference between the number of extreme events observed in the decades 1979–90 and 1991–2004 was assessed by testing the difference in the winter averages in the two periods (e.g. Spiegel and others, 2000). During 1979–90 the average number of negative (positive) extreme SIA_{IS} events was 2.75 (2.25) events per winter, with standard deviation 0.45 (0.75) events per winter. During 1991–2004 the average number of negative (positive) extreme SIA_{IS} events increased to 2.93 (2.93) events per winter, with standard deviation 0.73 (0.73) events per winter. Statistical significance (at 5% significance level) was observed only for the increase in the number of extreme positive SIA_{IS} events. Jacobs and Comiso (1997) showed changes in the interannual variability of sea-ice extent and a decrease of about 20% in the Amundsen and Bellingshausen sea-ice extent during two decades after 1973, particularly in the summer. They also showed that the interannual decrease of sea-ice extent in the oceans westward of the Antarctic Peninsula was negatively correlated with the air temperature at the surface, which increased at a rate of about $0.5^{\circ}C\,(10\,a)^{-1}$ since 1940. In the present study, however, we show that the mean number of extreme SIA_{IS} anomalies increased during the winter in the 1991–2004 period compared with the 1979–90 period. Nevertheless, the winter average persistence of negative (i.e. retraction) SIA_{IS} events also increased in the 1991–2004 period, resulting in changes in the characteristics of the persistence distribution as suggested by changes in the upper- and lower-quartile and interquartile ranges. The decrease in sea-ice extent on interannual timescales discussed by Jacobs and Comiso (1997) during summer, and by Zwally and others (2002) during winter, results from the interplay of phenomena occurring on several timescales. The present study suggests, however, that the persistence of the anomalous SIA retractions on intra-seasonal timescales in the winters of the last 14 years may have played a role for the reported seasonal trends.

Changes in the number of SIA_{IS} events after 1990 seem to be consistent with the study of Fogt and Bromwich (2006). They showed that the decadal variability of ENSO influenced the intensity of the teleconnection patterns in the 1990s similarly to the 1980s, mainly in the austral spring. They showed that the 1980s September–November teleconnection is weak due to the relationships between the Pacific–South American pattern associated with ENSO and the Southern Annular Mode. The significantly positive correlation between these two modes during September–November (also existing in December–February) in the 1990s amplifies the geopotential height and pressure anomalies over the South Pacific, strengthening the tropical–extratropical teleconnection identified through empirical orthogonal function analyses. It is possible therefore that the decadal variations in the number and persistence of SIA_{IS} extreme events observed after 1990 are linked to the mechanisms discussed by Fogt and Bromwich (2006). Moreover, Jones and Carvalho (2006) have shown that the number of Madden–Julian Oscillation events, the most significant intra-seasonal disturbance in the tropics (Madden and Julian, 1994), increased during the austral winter in the 1990s compared to the 1980s. The Rossby response of the Madden–Julian Oscillation plays an important role in modulating circulation in the extratropics, with subsequent influence on wave activity and phases of the Antarctic Oscillation (Carvalho and others, 2005).

https://doi.org/10.3189/172756408784700671 Published online by Cambridge University Press

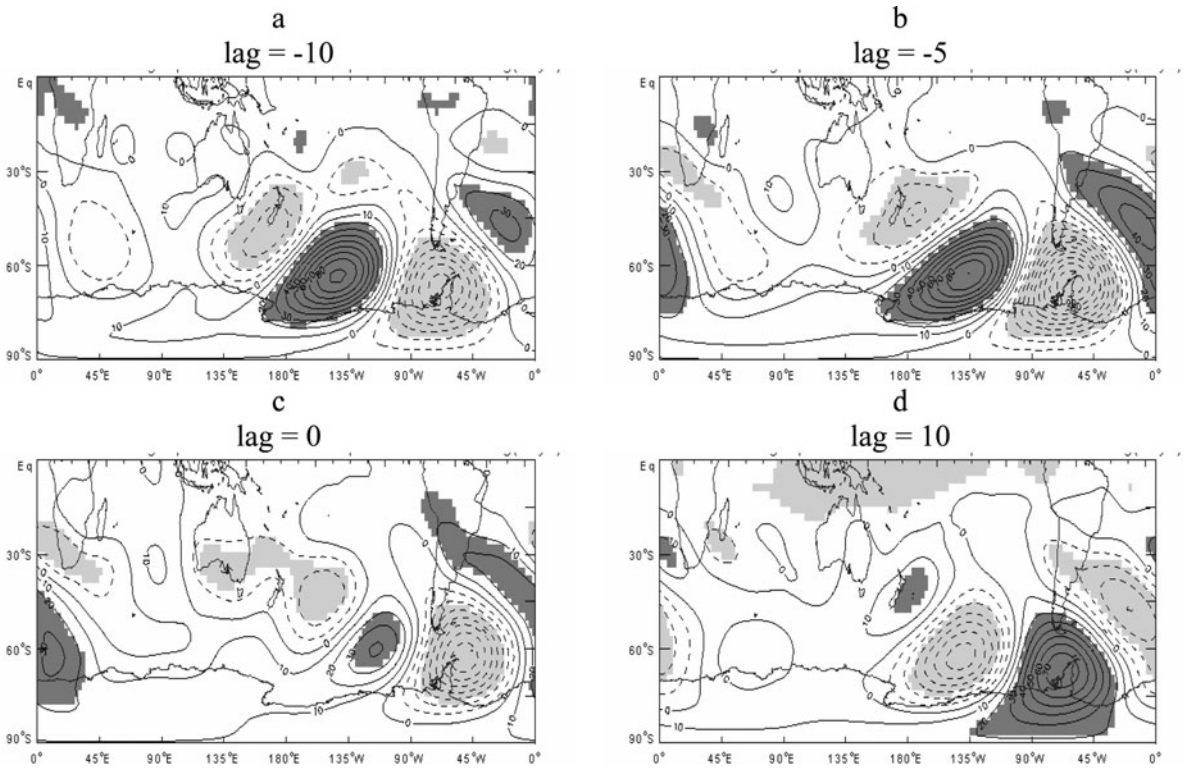

Fig. 5. Same as Figure 4, but for SIA_{IS} positive anomalies (DOF = 68).

The association of the propagation of atmospheric wave trains on intra-seasonal timescales with the SIA_{IS} extreme events is illustrated in the lag composites of Figures 4–8. The intra-seasonal wave train can be analogously compared to the ACW on interannual timescales (White and Peterson, 1996; Venegas and others, 2001). Both modes represent a coupled ocean–atmosphere system that can cause anomalies in the Antarctic SIA and extent. Lag composites illustrate different phases of propagation of the intra-seasonal atmospheric disturbances and are performed for SIA_{IS} negative and positive events separately. In Figures 4–8, lag = 0 means that the atmospheric field is observed along with the occurrence of the SIA_{IS}. Negative (positive) lag indicates that the feature observed leads (lags) the events by the number of days indicated at the top of each frame. All atmospheric variables are band-filtered on intra-seasonal timescales (20–100 days). The statistical significance of the mean anomaly is accessed by performing a *t* test at 5% significance level. We considered as independent events only those that are at least 2 days apart.

Figure 4 shows lag composites of the 200 hPa geopotential intra-seasonal anomalies ($H200_{IS}$) during extreme negative (ice retraction) SIA_{IS} events. A well-defined extratropical wave train can be observed 10–15 days before the events, lasting up to 10–15 days following the events. Around 20 days after (20 days before) the events, the wave pattern weakens (not shown). Simmonds (2003) pointed out that the Antarctic Peninsula, which includes the Weddell and Bellingshausen Seas, is the region in the SH that is most subjected to the influence of atmospheric systems that develop in mid-latitudes, including those with longitudinal propagation. For lag = –10 days (Fig. 4a), a wavenumber-2 pattern in the $H200_{IS}$ is clearly observed in the mid-latitudes of the South Pacific extending towards the South Atlantic. Positive geopotential anomalies are observed west of the Antarctic Peninsula and around New Zealand. For lag = –5 days (Fig. 4b), positive geopotential anomalies intensify over the Amundsen and Bellingshausen Seas, and on lag = 0 (Fig. 4c) this centre moves towards the eastern Antarctic Peninsula. It is interesting to notice also the influence of the wave train upon the subtropics, particularly over La Plata basin in South America and southern Africa on lags –5 and 0, when a zonal wavenumber 3 becomes evident. By lag = 10 days (Fig. 4d), negative $H200_{IS}$ anomalies are observed over the Antarctic Peninsula as the wave train moves eastward, with spatial distribution of anomalies almost opposite to what is observed for lag = –10 days (Fig. 4a). The intra-seasonal wave train presents a coherent pattern of geopotential and circulation from low to high levels (not shown).

The occurrence of positive SIA_{IS} anomalies in the Amundsen and Bellingshausen Seas also depends on the phases of propagation of the mid-latitudes intra-seasonal wave train. Figure 5 illustrates this dependence by showing $H200_{IS}$ lag composites obtained with respect to the occurrence of extreme intra-seasonal SIA_{IS} positive anomalies (i.e. extreme expansion of the sea ice on intra-seasonal timescales). For lag = –10 days (Fig. 5a) the wave pattern resembles that observed for lag = 10 days for negative SIA_{IS} anomalies (Fig. 4a). That is, negative geopotential anomalies are observed over the Antarctic Peninsula, particularly over the Amundsen and Bellingshausen Seas for lags of –5 to 0 days (Fig. 5a and c), being replaced by positive anomalies for lags of 5–10 days (Fig. 5d). These negative geopotential height anomalies are collocated with southerly $V850_{IS}$ anomalies (not shown), which implies southerly advection of cold air and expansion of the ice sheet. It is important to notice that not all extreme positive (negative) SIA_{IS} anomalies are necessarily followed by extreme negative (positive) anomalies as the wave train moves eastward. The

https://doi.org/10.3189/172756408784700671 Published online by Cambridge University Press

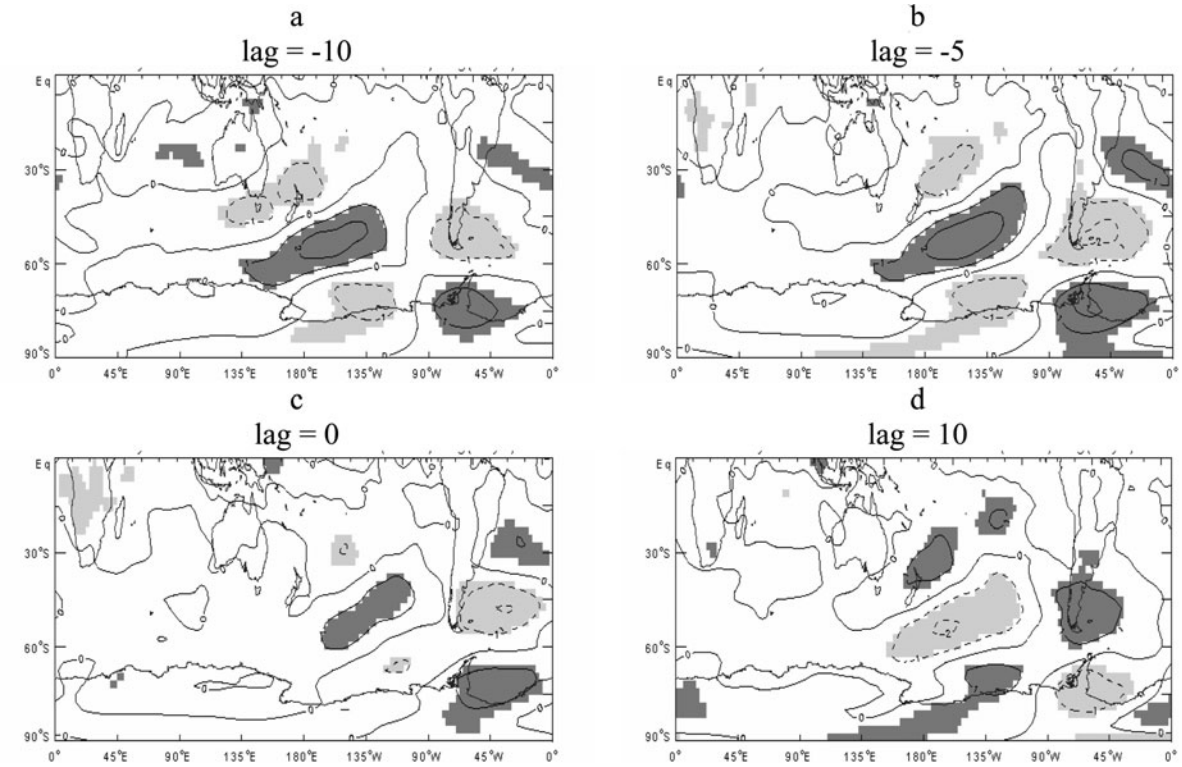

Fig. 6. Same as Figure 4, but for the zonal wind intra-seasonal anomaly ($m\,s^{-1}$) at 850 hPa ($U850_{IS}$). Solid (dashed) lines indicate positive (negative) anomalies starting at $5\,m\,s^{-1}$ ($-5\,m\,s^{-1}$) with $1\,m\,s^{-1}$ interval. DOF = 70.

occurrence of extreme variations in the ice may depend on the interaction of several scales and local factors. Moreover, variations in the Southern Ocean currents, sea surface temperature and salinity (Gordon and Taylor 1975; Gordon 1981; Lohmann and Gerdes 1998), not explored in the present study, can play an important role in the sea-ice variability on intra-seasonal timescales.

Lag composites of zonal wind intra-seasonal anomalies at 850 hPa ($U850_{IS}$) associated with extreme negative SIA_{IS} anomalies are shown in Figure 6. The wavenumber-3 pattern is already evident 10 days before the event (Fig. 6a) and resembles the tropical–extratropical teleconnection patterns suggested in Mo and Paegle (2001). Westerly intra-seasonal wind anomalies are observed west of the Antarctic Peninsula for lag = –10 days (Fig. 6a) to lag = 0 (Fig. 6c). The strongest anomalies are observed preceding the events 10–5 days. For lag = 0 (Fig. 6c), $U850_{IS}$ weakens near the Antarctic Peninsula, and for lag = 10 days (Fig. 6d) easterly anomalies replace the westerly anomalies, indicating a wave phase opposite to that observed for lag = –10 days (Fig. 6a).

Lag composites of intra-seasonal anomalies of the meridional wind component at 850 hPa ($V850_{IS}$) and skin temperature (SKT_{IS}) are shown in Figures 7 and 8, respectively. For lag = –10 days (Fig. 7a) northerly $V850_{IS}$ anomalies are observed west of the Antarctic Peninsula, collocated with the Amundsen and Bellingshausen Seas. The low-level northerly components bring warm air to the west of the peninsula, and the net result is the increase of SKT_{IS} anomalies (Fig. 8a) due to the increase of sea surface temperature combined with the poleward retraction of the ice limits. Conversely, southerly $V850_{IS}$ anomalies are observed along with a decrease in SKT_{IS} anomalies for all lags. Northerly $V850_{IS}$ anomalies preceding negative SIA_{IS} anomalies persist and intensify from lag = –10 days to lag = –5 days (Fig. 7b), which is followed by an increase in SKT_{IS} anomalies (Fig. 8b) over the Amundsen and Bellingshausen Seas. $V850_{IS}$ and SKT_{IS} anomalies weaken for lag = 0 (Figs 7c and 8c), and an opposite phase is observed for lag = 10 (Figs 7d and 8d). The eastward propagation of the SIA_{IS} anomalies has been identified also by Baba and others (2006).

CONCLUSIONS

The spectral density of the daily Amundsen and Bellingshausen SIA for 1979–2004 showed several statistically significant peaks on intra-seasonal timescales within the 20–100 day band. Some peaks occur at longer timescales than have been observed before (Baba and Wakatsuchi, 2001; Baba and others, 2006). Extreme variation in the band-filtered SIA_{IS}, defined according to the upper and lower quartiles of the SIA_{IS}, occurs every winter season. However, the proportion of events that cause extreme expansion or retraction of SIA varies from year to year. The total number of events causing extreme intra-seasonal variations in the SIA is about one to four per winter. There is some indication of an increase in the average number of events per year in the 1991–2004 period compared to 1979–90. Statistical significance is found (at 5% significance level) for the increase in the average number of extreme positive (expansion) SIA_{IS} events per year. On the other hand, the upper quartile of the persistence (defined as consecutive days with extreme anomalies) of extreme negative (retraction) SIA_{IS} has also increased in the last 14 years. The combined effect of a larger number of SIA_{IS} events (either positive or negative) and the increase in the upper quartile of the persistence of ice retraction on intra-seasonal timescales, particularly during the 1991, 1996 and 2001 winters, may

https://doi.org/10.3189/172756408784700671 Published online by Cambridge University Press

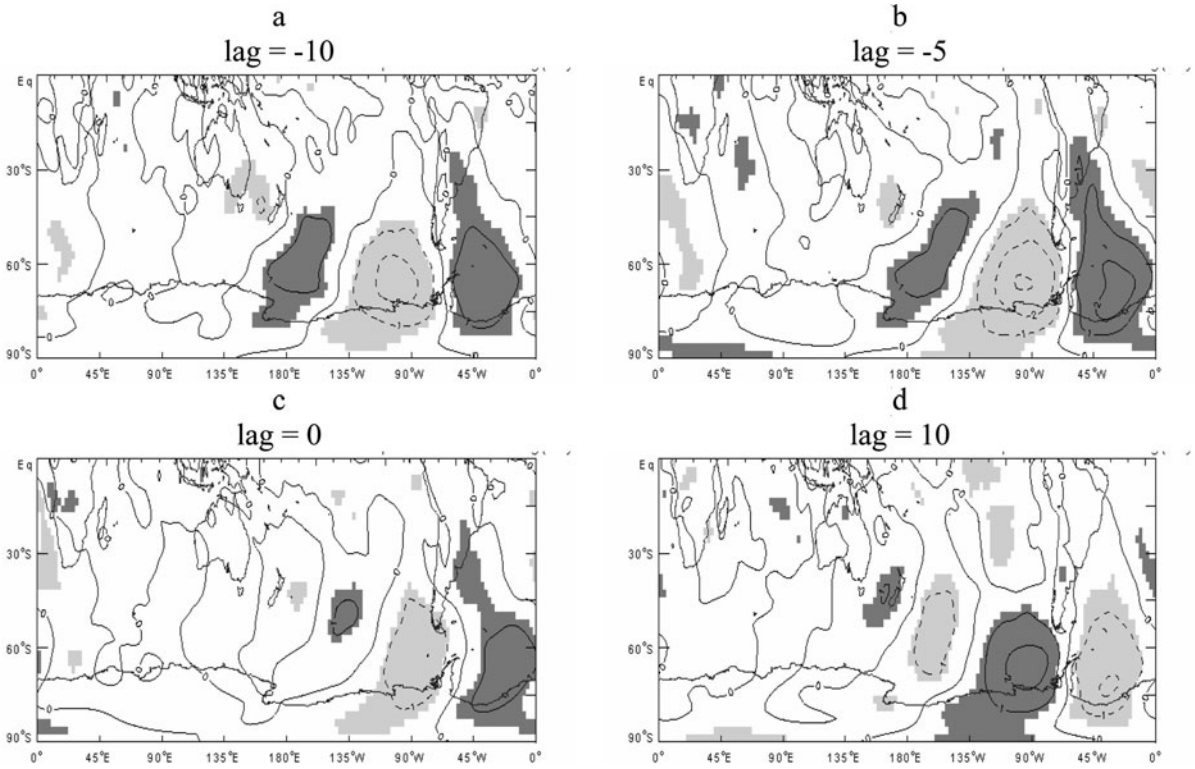

Fig. 7. Same as Figure 6, but for the intra-seasonal meridional wind anomaly ($m\,s^{-1}$) at 850 hPa ($V850_{IS}$).

have played a role for the winter SIA trends in the last decade. The decadal variation of SIA_{IS} has observational support in the studies of Fogt and Bromwich (2006) and Jones and Carvalho (2006).

Atmospheric disturbances on intra-seasonal timescales that propagate to the SH extratropics as wave trains have important impacts on the occurrence of extreme SIA_{IS}. We show that these disturbances appear as a wave 2–3 in the

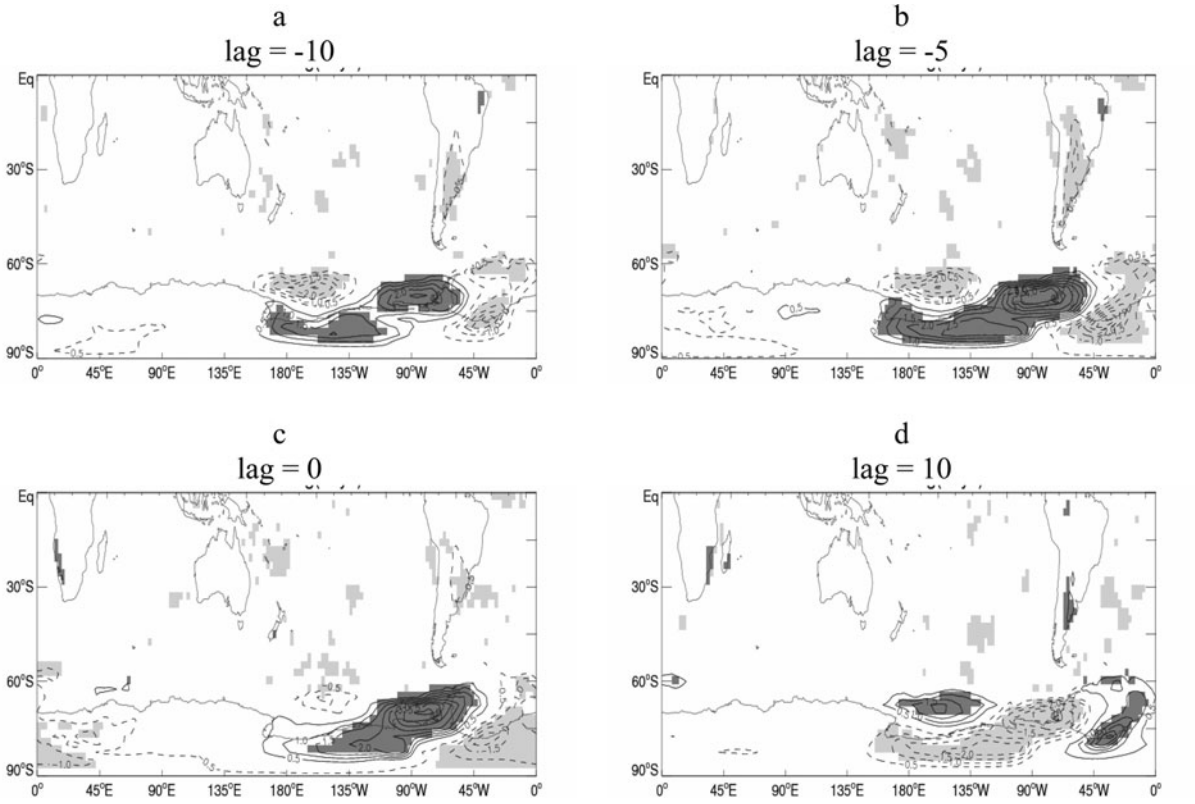

Fig. 8. Same as Figure 7, but for skin temperature (K) intra-seasonal anomaly (SKT_{IS}). Solid (dashed) lines indicate positive (negative) anomalies starting at 4 K (–4 K) with 0.5 K interval. DOF = 70.

https://doi.org/10.3189/172756408784700671 Published online by Cambridge University Press

geopotential height and circulation. The origin of these disturbances is still debatable, but their spatio-temporal characteristics suggest the importance of tropical–extratropical teleconnections on intra-seasonal timescales. The occurrence of extreme retraction or expansion of the Amundsen and Bellingshausen SIA depends on the phase of propagation of the wave train and the persistence of the event. Nevertheless, the occurrence of extreme retraction in one phase of the wave does not always imply extreme expansion during the other phase, due to local factors, ocean currents and many other causes not explored in the present study.

ACKNOWLEDGEMENTS

We thank NCEP/NCAR for the re-analysis and NSIDC for sea-ice area data. This research was funded by FAPESP-04/11808-0 (F.U.F. Lima) and CNPq Proc 474033/2004-0 (L.M.V. Carvalho).

REFERENCES

Baba, K. and M. Wakatsuchi. 2001. Eastward propagation of the intraseasonal variability of sea ice and the atmospheric field in the marginal ice zone in the Antarctic. *Geophys. Res. Lett.,* **28**(19), 3669–3672.

Baba, K., S. Minobe, N. Kimura and M. Wakatsuchi. 2006. Intra-seasonal variability of sea-ice concentration in the Antarctic with particular emphasis on wind effect. *J. Geophys. Res.,* **111**(C12), C12023. (10.1029/2005JC003052.)

Carvalho, L.M.V., C. Jones and T. Ambrizzi. 2005. Opposite phases of the Antarctic Oscillation and relationships with intraseasonal to interannual activity in the tropics during the austral summer. *J. Climate,* **18**(5), 702–718.

Fogt, R.L. and D.H. Bromwich. 2006. Decadal variability of the ENSO teleconnection to the high-latitude South Pacific governed by coupling with the Southern Annular Mode. *J. Climate,* **19**(6), 979–997.

Gordon, A.L. 1981. Seasonality of Southern Ocean ice. *J. Geophys. Res.,* **86**(C5), 4193–4197.

Gordon, A.L. and H.W. Taylor. 1975. Seasonal change of Antarctic sea ice cover. *Science,* **187**(4174), 346–347.

Harangozo, S.A. 2000. A search for ENSO teleconnections in the west Antarctic Peninsula climate in austral winter. *Int. J. Climatol.,* **20**(6), 663–679.

Helms, H. 1967. Fast Fourier transform method of computing difference equations and simulating filters. *IEEE Trans. Audio Electroacoust.,* **15**(2), 85–90.

Jacobs, S.S. and J.C. Comiso. 1997. Climate variability in the Amundsen and Bellingshausen seas. *J. Climate,* **10**(4), 697–709.

Jones, C. and L.M.V. Carvalho. 2006. Changes in the activity of the Madden–Julian oscillation during 1958–2004. *J. Climate,* **19**(24), 6353–6370.

Kalnay, E. *and 21 others*. 1996. The NCEP/NCAR 40-year reanalysis project. *Bull. Am. Meteorol. Soc.,* **77**(3), 437–471.

Lima, F.U.F. 2007. Extreme intra-seasonal variability of the Antarctic sea ice and relationships with the atmosphere circulation. (Master's thesis, University of São Paulo.)

Lohmann, G. and R. Gerdes. 1998. Sea ice effects on the sensitivity of the thermohaline circulation. *J. Climate,* **11**(11), 2789–2803.

Madden, R.A. and P.R. Julian. 1994. Observations of the 40–50-day tropical oscillation – a review. *Mon. Weather Rev.,* **122**(5), 814–837.

Mo, K.C. and J.N. Paegle. 2001. The Pacific–South American modes and their downstream effects. *Int. J. Climatol.,* **21**(10), 1211–1229.

Renwick, J.A. 2002. Southern Hemisphere circulation and relations with sea ice and sea surface temperature. *J. Climate,* **15**(21), 3058–3068.

Simmonds, I. 2003. Regional and large-scale influences on Antarctic Peninsula climate. *In* Domack, E., A. Leventer, A. Burnett, R. Bindschadler, P. Convey and M. Kirby, *eds. Antarctic Peninsula climate variability: historical and paleoenvironmental perspectives*. Washington, DC, American Geophysical Union. (Antarctic Research Series 79.)

Simmonds, I. and T.H. Jacka. 1995. Relationships between the interannual variability of Antarctic sea ice and the Southern Oscillation. *J. Climate,* **8**(3), 637–647.

Spiegel, M.R., J.J. Schiller and A.L. Srinivasan. 2000. *Schaum's outline of probability and statistics. Second edition*. New York, McGraw-Hill.

Venegas, S.A., M.R. Drinkwater and G. Shaffer. 2001. Coupled oscillations in Antarctic sea ice and atmosphere in the South Pacific sector. *Geophys. Res. Lett.,* **28**(17), 3301–3304.

Walker, G.T. 1923. Correlation in seasonal variations of weather, VIII. A preliminary study of world weather. *Mem. Indian Meteorol. Dept,* **24**(4), 75–131.

Walker, G.T. 1924. Correlation in seasonal variation of weather, IX: a further study of world weather. *Mem. Indian Meteorol. Dept,* **24**(9), 275–332.

White, W.B. and R.G. Peterson. 1996. An Antarctic circumpolar wave in surface pressure, wind, temperature and sea-ice extent. *Nature,* **380**(6576), 699–702.

Yuan, X. and D.G. Martinson. 2001. The Antarctic dipole and its predictability. *Geophys. Res. Lett.,* **28**(18), 3609–3612.

Zwally, H.J., J.C. Comiso, C.L. Parkinson, D.J. Cavalieri and P. Gloersen. 2002. Variability of Antarctic sea ice 1979–1998. *J. Geophys. Res.,* **107**(C5), 3041. (10.1029/2000JC000733.)

https://doi.org/10.3189/172756408784700671 Published online by Cambridge University Press